Counter Anion Effect on the Spin-crossover Behaviors of Two-dimensional Fe(II) Complexes with a Tripod Ligand Containing Three Imidazoles

S. Iijima,*,[a] H. Hagiwara,[b] H. Torigoe,[b] and N. Matsumoto[b]

[a]*National Institute of Advanced Industrial Science and Technology (AIST), Tsukuba, Ibaraki 305-8566, Japan*
[b]*Department of Chemistry, Kumamoto University, Kurokami, Kumamoto 860-8555, Japan*

^{57}Fe Mössbauer spectroscopy has provided detailed information about the low-spin/high-spin transition in two types of two-dimensional Fe(II) complexes, $[Fe^{II}H_3L^{Me}][Fe^{II}L^{Me}]X$ ($X^- = BF_4^-$, ClO_4^-, PF_6^-, NO_3^-) **1–4** and $[Fe^{II}H_3L^{Me}]Cl\cdot X$ ($X^- = PF_6^-$, AsF_6^-, SbF_6^-) **5–7**, where H_3L^{Me} denotes a hexadentate N_6 tripod-like ligand containing three imidazole groups, tris[2-(((2-methylimidazol-4-yl)methylidene)amino)ethyl]amine. The molar fraction of high-spin Fe^{II} versus total Fe^{II} (γ_{HS}) was estimated from Mössbauer area intensities of each compound in different temperatures. The γ_{HS}-T plots for **1–4** indicated that these compounds exhibit a two-step spin crossover corresponding to (LS-$[Fe^{II}H_3L^{Me}]^{2+}$ + LS-$[Fe^{II}L^{Me}]^-$) $\leftrightarrow$ (HS-$[Fe^{II}H_3L^{Me}]^{2+}$ + LS-$[Fe^{II}L^{Me}]^-$) $\leftrightarrow$ (HS-$[Fe^{II}H_3L^{Me}]^{2+}$ + HS-$[Fe^{II}L^{Me}]^-$). The larger size of the counter anion separated the first and second spin crossover transitions in the $[Fe^{II}H_3L^{Me}][Fe^{II}L^{Me}]X$ system well. A variety of γ_{HS}-T curves depending on the counter anion was observed for $[Fe^{II}H_3L^{Me}]Cl\cdot X$. It was suggested that a smaller counter anion stabilizes the 1/2(LS-$[Fe^{II}H_3L^{Me}]^{2+}$ + HS-$[Fe^{II}H_3L^{Me}]^{2+}$) state in this system.

1. Introduction

Spin-crossover (SCO) between the low-spin (LS) and high-spin (HS) states is observed in some octahedral $3d^n$ ($4 \leq n \leq 7$) metal complexes, and SCO is a representative example of molecular bistability.[1,2] The two spin states are interconvertible by physical perturbations (a change in temperature, pressure, irradiation with light, etc.), and therefore, the SCO metal complexes have attracted increased attention with regard to potential applications to new electronic devices such as molecular memories, switches, and visual displays. Matsumoto et al. and Kojima et al. have extensively investigated a series of iron complexes with N_6 tripod ligands containing three imidazole groups, H_3L^R = tris[2-(((2-R-imidazol-4-yl)methylidene)amino)ethyl]amine.[3–8] The H_3L^R-Fe^{II} and -Fe^{III} complexes exhibit a wide variety of SCO transitions with different features in the steepness and multi-step nature, hysteresis, frozen-in effect, and so on. Combined with cryomagnetic measurements, ^{57}Fe Mössbauer spectroscopy provides important information about SCO phenomena in iron compounds; essentially, the HS/LS ratio of such a complex is derived directly from the Mössbauer area intensities at different temperatures.[1,2] This article reports detailed temperature-dependences of Mössbauer spectra for two series of Fe(II) complexes $[Fe^{II}H_3L^{Me}][Fe^{II}L^{Me}]X$ ($X^- = BF_4^-$, ClO_4^-, PF_6^-, NO_3^-) **1–4** and $[Fe^{II}H_3L^{Me}]Cl\cdot X$ ($X^- = PF_6^-$, AsF_6^-, SbF_6^-) **5–7** to understand systematically the counter anion effect on the SCO behaviors of these two-dimensional (2D) systems, where H_3L^{Me} denotes tris[2-(((2-methylimidazol-4-yl)methylidene)amino)ethyl]amine, and the chemical structures of $[Fe^{II}H_3L^{Me}]^{2+}$ and $[Fe^{II}L^{Me}]^-$ moieties are shown in Figure 1. Part of this work has been reported previously.[5,8]

2. Experimental

The procedures for preparing compounds **1–7** were reported previously.[5,8]
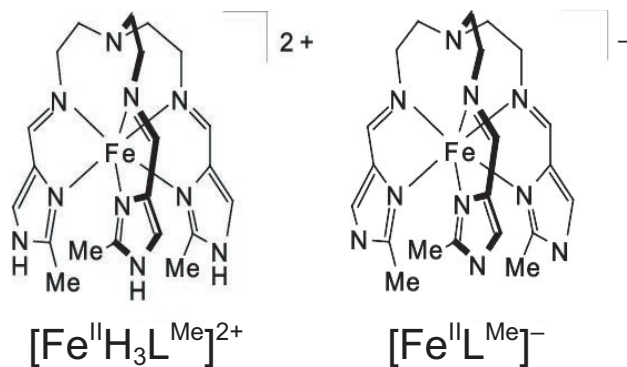
The ^{57}Fe Mössbauer spectra were recorded using a Wissel

Figure 1. Molecular structures of $[Fe^{II}H_3L^{Me}]^{2+}$ and $[Fe^{II}L^{Me}]^-$.

1200 spectrometer and a proportional counter. ^{57}Co(Rh) moving in a constant acceleration mode was used as radioactive source. The calculated lines were obtained by least-squares fitting to Lorentzian peaks. The isomer shifts are reported relative to metallic iron foil. The sample temperature was controlled by a Heli-tran liquid transfer refrigerator (Air Products and Chemicals, Inc.) within an accuracy of ±0.5 K.

3. Results and Discussion

$[Fe^{II}H_3L^{Me}][Fe^{II}L^{Me}]X$ complexes **1–4** assume a homochiral 2D sheet structure, in which the capped tripodlike ligands $[Fe^{II}H_3L^{Me}]^{2+}$ and $[Fe^{II}L^{Me}]^-$ are alternately arrayed in an up-and-down mode and are linked by the imidazole-imidazolate hydrogen bonds.[5] The counter anions are located between the 2D sheets. The ^{57}Fe Mössbauer spectra were investigated in the 78–298 K range for **1–3** and in the 4.2–298 K range for **4**. The sample was initially rapidly cooled to 78 K for **1–3** and 4.2 K for **4**, (within 3 min from room temperature), and the spectra were measured at selected temperatures in the warming mode, and then cooling mode.

The representative spectra of **1** ($X^- = BF_4^-$) in the warming mode are shown in Figure 2. At 78 K (Figure 2(d)), the spectrum consisted of a single quadrupole doublet assignable to LS-

*Corresponding author. E-mail: s.iijima@aist.go.jp. Fax: +81-29-861-6177.
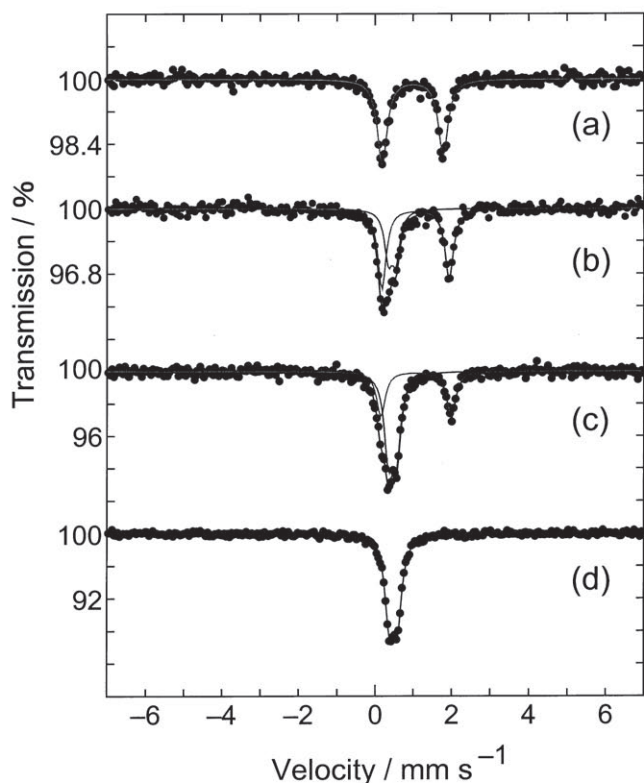
Figure 2. Selected ^{57}Fe Mössbauer spectra of $[Fe^{II}H_3L^{Me}][Fe^{II}L^{Me}]BF_4$ (**1**) at (a) 298 K, (b) 200 K, (c) 160 K, and (d) 78 K in the warming mode.

TABLE 1: Mössbauer parameters for $[Fe^{II}H_3L^{Me}][Fe^{II}L^{Me}]$ BF$_4$ (1) in the warming mode

T / K	δ^a / mm·s^{-1}	ΔE_Q / mm s^{-1}	Γ^b / mm s^{-1}	Relative area / %
298	0.98	1.60	0.31	100
275	1.01	1.63	0.31	100
250	1.02	1.66	0.31	93
	0.47	0.20	0.25	7
220	1.02	1.74	0.29	82
	0.46	0.20	0.25	18
200	1.06	1.76	0.27	63
	0.45	0.20	0.25	37
180	1.05	1.81	0.26	46
	0.44	0.21	0.26	54
170	1.07	1.81	0.26	42
	0.45	0.21	0.28	58
160	1.07	1.84	0.28	38
	0.45	0.21	0.26	62
140	1.06	1.87	0.26	17
	0.47	0.20	0.26	83
120	1.02	2.16	0.29	5
	0.47	0.20	0.28	95
100	0.48	0.21	0.26	100
78	0.48	0.21	0.28	100

^{a}Isomer shift data are reported to iron foil.
^{b}Full width at half-height.

Fe^{II} (isomer shift δ = 0.48 mm/s and quadrupole splitting ΔE_Q = 0.21 mm/s). Although two types of iron species, $[Fe^{II}H_3L^{Me}]^{2+}$ and $[Fe^{II}L^{Me}]^-$, would be expected, the Mössbauer spectra did not distinguish them. A large extent of charge delocalization between $[Fe^{II}H_3L^{Me}]^{2+}$ and $[Fe^{II}L^{Me}]^-$ units probably arises from the extended imidazole-imidazolate hydrogen bond network, and it would yield the undistinguishable quadrupole doublets. The Mössbauer spectrum of **1** at 298 K exhibited a single doublet with large δ (0.98 mm/s) and ΔE_Q (1.60 mm/s), which are characteristic of HS-Fe^{II} (Figure 2(a)). Between 120
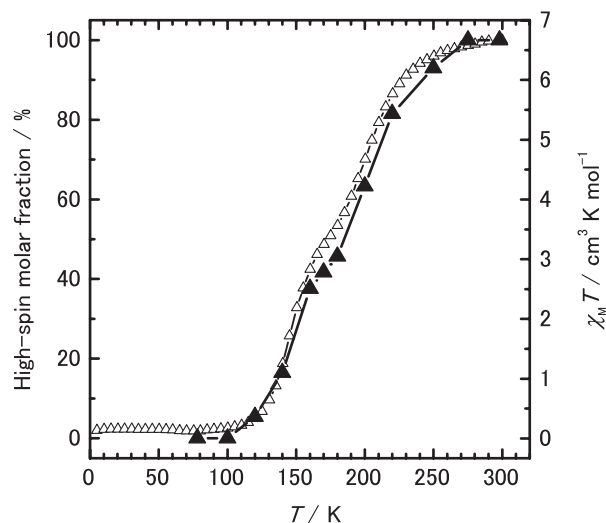

Figure 3. Temperature dependences of the molar fraction of HS versus total Fe^{II}, γ_{HS} (▲), and $\chi_M T$ (△) for $[Fe^{II}H_3L^{Me}][Fe^{II}L^{Me}]BF_4$ (**1**) in the warming mode. The γ_{HS} value was obtained by deconvolution analysis of the Mössbauer spectrum at each temperature; χ_M = molar magnetic susceptibility.

and 250 K, both of the LS-Fe^{II} and the HS-Fe^{II} absorptions were observed in the spectra (Figures 2(b) and 2(c)). A deconvolution analysis of the spectrum at each temperature was carried out to determine the molar fraction of the HS-Fe^{II} versus total Fe^{II} (γ_{HS}). The resulting Mössbauer parameters are summarized in Table 1. The γ_{HS} derived from Mössbauer area intensities are plotted against T in Figure 3, along with the magnetic susceptibility (χ_M) data reported.[5] The temperature dependence of γ_{HS} was essentially in agreement with that of $\chi_M T$ for **1**. The γ_{HS}-T curve had a plateau region at ca. 160–180 K with the γ_{HS} value close to 0.5, indicating a two-step SCO process; $(LS-[Fe^{II}H_3L^{Me}]^{2+} + LS-[Fe^{II}L^{Me}]^-) \leftrightarrow (HS-[Fe^{II}H_3L^{Me}]^{2+} + LS-[Fe^{II}L^{Me}]^-) \leftrightarrow (HS-[Fe^{II}H_3L^{Me}]^{2+} + HS-[Fe^{II}L^{Me}]^-)$. It is probable that the spin transition temperature ($T_{1/2}$) of $[Fe^{II}H_3L^{Me}]^{2+}$ is lower than that of $[Fe^{II}L^{Me}]^-$, because the deprotonated L^{Me} ligand would supply a stronger ligand field to Fe^{II} compared to the neutral H$_3$L^{Me} ligand. From the γ_{HS}-T curve, $T_{1/2}$ values were estimated to be ca. 150 K for $[Fe^{II}H_3L^{Me}]^{2+}$ and 210 K for $[Fe^{II}L^{Me}]^-$, the temperatures where γ_{HS} = 0.25 and 0.75, respectively. The Mössbauer spectra of **1** in the warming mode and in the cooling mode were almost the same at each temperature.

The γ_{HS} values of **2–4** derived from their Mössbauer spectra in the warming mode are plotted against T in Figure 4, together with the γ_{HS} data of **1** for comparison. Compounds **2** (X$^-$ = ClO$_4^-$) and **3** (X$^-$ = PF$_6^-$) gave γ_{HS}-T curves closely similar to that of **1**, showing a two-step SCO. However, the intervals of the $T_{1/2}$ values for $[Fe^{II}H_3L^{Me}]^{2+}$ and $[Fe^{II}L^{Me}]^-$ ($\Delta T_{1/2}$), were different to each other; $\Delta T_{1/2} \approx$ 60 K, 70 K, 90 K for **1**, **2**, **3**, respectively. A clear plateau region is observable in the γ_{HS}-T curve of **3** between ca. 180–220 K, due to the large $\Delta T_{1/2}$ value of this compound. The molecular volumes, V, of the counter anions were reported by using quantum chemical calculation as follows: 53.4 Å^3 for BF$_4^-$, 54.4 Å^3 for ClO$_4^-$, and 73.0 Å^3 for PF$_6^-$.[8] It is suggested that the $\Delta T_{1/2}$ depends on the size of the counter anion. The γ_{HS}-T curve of **4** (X$^-$ = NO$_3^-$) showed a small hump below ca. 50 K, which is ascribable to frozen-in effect; such a hump was not observed in the γ_{HS}-T curve obtained by the cooling mode measurements (data not shown), while a somewhat large γ_{HS} (0.24–0.26) still remained at 4.2–50 K for **4**.
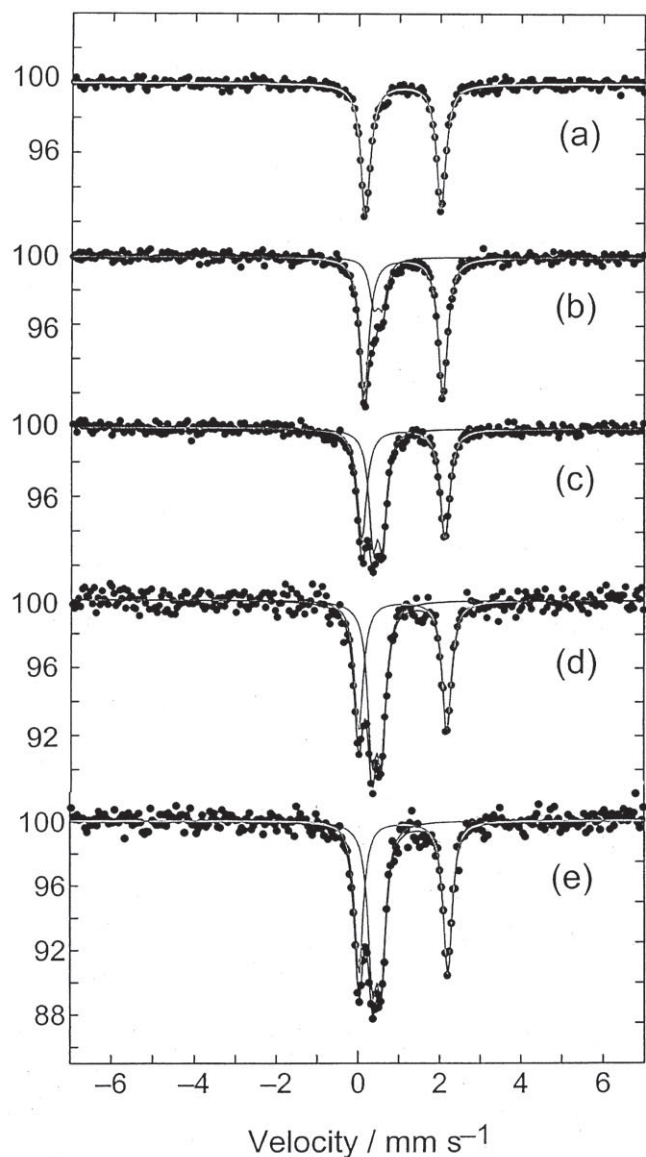
The general crystal structure of $[Fe^{II}H_3L^{Me}]Cl·X$ complexes **5–7** consists of a 2D extended network constructed by NH···Cl$^-$ hydrogen bonds between Cl$^-$ and imidazole NH groups of three neighboring $[Fe^{II}H_3L^{Me}]^{2+}$ ions.[8] The anion X occupies the
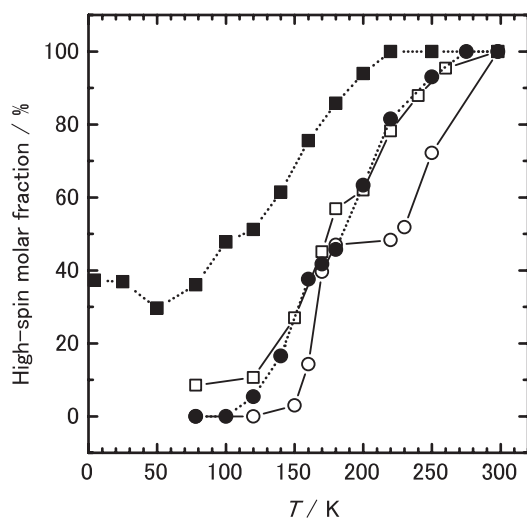
Figure 4. Molar fraction of HS versus total Fe^{II}, γ_{HS}-T, for $[Fe^{II}H_3L^{Me}][Fe^{II}L^{Me}]BF_4$ (**1**) (●), $[Fe^{II}H_3L^{Me}][Fe^{II}L^{Me}]ClO_4$ (**2**) (□), $[Fe^{II}H_3L^{Me}][Fe^{II}L^{Me}]PF_6$ (**3**) (○), and $[Fe^{II}H_3L^{Me}][Fe^{II}L^{Me}]NO_3$ (**4**) (■), obtained by deconvolution analysis of the Mössbauer spectra in the warming mode.
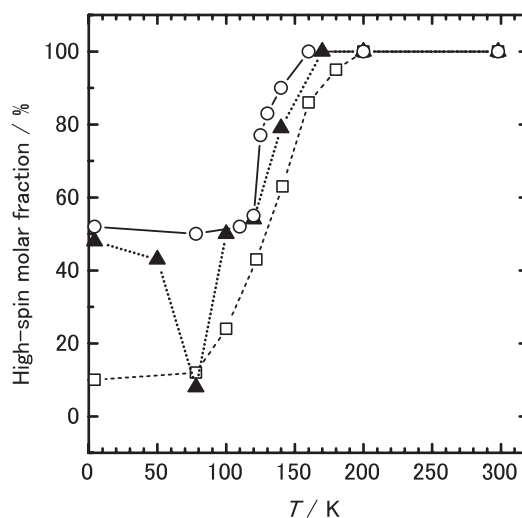
Figure 6. Molar fraction of HS versus total Fe^{II}, γ_{HS}-T, for $[Fe^{II}H_3L^{Me}]Cl \cdot PF_6$ (**5**) (○), $[Fe^{II}H_3L^{Me}]Cl \cdot AsF_6$ (**6**) (▲), and $[Fe^{II}H_3L^{Me}][Fe^{II}L^{Me}]SbF_6$ (**7**) (□) obtained by deconvolution analysis of the Mössbauer spectra in the warming mode.

space between the 2D sheets. The ^{57}Fe Mössbauer spectra of **5**–**7** were measured in the 4.2–298 K range in the warming mode after rapid cooling to 4.2 K, and then in the cooling mode. A variety of SCO behaviors depending on the counter anion was revealed in this 2D system.

Selected Mössbauer spectra of **5** ($X^- = PF_6^-$) obtained in the warming mode are shown in Figure 5. Between 4.2 K and 110 K, both of LS-Fe^{II} ($\delta = 0.47$ mm/s and $\Delta E_Q = 0.23$ mm/s at 78 K) and HS-Fe^{II} ($\delta = 1.10$ mm/s and $\Delta E_Q = 2.16$ mm/s at 78 K) absorptions were observed in the area intensity ratio of about 1:1 (Figures 5(d) and 5(e)). On elevating the temperature above 120 K, the HS-Fe^{II} absorption increased at the expense of the LS-Fe^{II} absorption (Figures 5(b) and 5(c)), and the LS-Fe^{II} component disappeared at 160 K (Figure 5(a)). The γ_{HS} values derived from Mössbauer area intensities for **5** in the warming mode are plotted against T in Figure 6, along with the γ_{HS} data for **6** and **7** mentioned later. The γ_{HS}-T curve of **5** indicates that $1/2(LS-[Fe^{II}H_3L^{Me}]^{2+} + HS-[Fe^{II}H_3L^{Me}]^{2+})$ state is stable for **5** in the lower temperature region. The Mössbauer spectra of **5** in the warming mode and in the cooling mode were nearly the same at each temperature.

The γ_{HS}-T curve of **6** ($X^- = AsF_6^-$) in the warming mode, shown in Figure 6, exhibited a plateau region at ca. 100–120 K with the γ_{HS} value close to 0.5, indicating a two-step SCO process; LS-$[Fe^{II}H_3L^{Me}]^{2+} \leftrightarrow 1/2(LS-[Fe^{II}H_3L^{Me}]^{2+} + HS-[Fe^{II}H_3L^{Me}]^{2+}) \leftrightarrow HS-[Fe^{II}H_3L^{Me}]^{2+}$. The hump below 50 K in the γ_{HS}-T curve is ascribable to frozen-in effect, because the hump disappeared in the cooling mode measurements. On the other hand, compound **7** ($X^- = SbF_6^-$) afforded a γ_{HS}-T curve corresponding to a one-step LS-$[Fe^{II}H_3L^{Me}]^{2+} \leftrightarrow HS-[Fe^{II}H_3L^{Me}]^{2+}$ transition with $T_{1/2} = 130$ K, as shown in Figure 6. A small HS-Fe^{II} absorption ($\gamma_{HS} = 0.08$–0.12) was observed between 4.2 K and 78 K for **7** both in the warming and cooling modes. The above SCO behaviors of **5**–**7** suggests that the increase in the size of the counter anion in the series PF_6^-, AsF_6^-, and SbF_6^- ($V = 73.0$ Å^3, 78.5 Å^3, and 88.7 Å^3, respectively)[8] leads a decrease in the stabilization of $1/2(LS-[Fe^{II}H_3L^{Me}]^{2+} + HS-[Fe^{II}H_3L^{Me}]^{2+})$ state. There is the possibility that the optimum size of the counter anion to stabilize the intermediate spin transition states is around that of PF_6^-, commonly in these 2D systems $[Fe^{II}H_3L^{Me}][Fe^{II}L^{Me}]X$ and $[Fe^{II}H_3L^{Me}]Cl \cdot X$. For clarifying this point, it would be needed to investigate a further variety of $[Fe^{II}H_3L^{Me}][Fe^{II}L^{Me}]X$ and $[Fe^{II}H_3L^{Me}]Cl \cdot X$ salts by the use of ^{57}Fe Mössbauer spectroscopy.

Figure 5. Selected ^{57}Fe Mössbauer spectra of $[Fe^{II}H_3L^{Me}]Cl \cdot PF_6$ (**5**) at (a) 160 K, (b) 125 K, (c) 120 K, (d) 78 K, and (e) 4.2 K in the warming mode.

By applying ^{57}Fe Mössbauer spectroscopy, this paper has revealed that the counter anion size is one of the important factors governing the SCO behavior for two types of 2D iron complexes, [Fe^{II}H$_3$L^{Me}][Fe^{II}L^{Me}]X and [Fe^{II}H$_3$L^{Me}]Cl·X. It is probable that the anion size affects the interaction between the 2D sheets in the crystal lattice of each type of complexes, which controls the stabilities of the intermediate spin transition states, (HS-[Fe^{II}H$_3$L^{Me}]$^{2+}$ + LS-[Fe^{II}L^{Me}]$^-$) in [Fe^{II}H$_3$L^{Me}][Fe^{II}L^{Me}]X and 1/2(LS-[Fe^{II}H$_3$L^{Me}]$^{2+}$ + HS-[Fe^{II}H$_3$L^{Me}]$^{2+}$) in [Fe^{II}H$_3$L^{Me}]Cl·X. The results obtained in the present study would be useful for experimental and theoretical investigation of the origin of multistep spin transition.[1,9–12]

References

(1) P. Gütlich and H. A. Goodwin, *Spin Crossover in Transition Metal Compounds I*, Topics in Current Chemistry, Vol. 233, Springer, New York (2004).

(2) E. Köndig, Struct. Bonding (Berlin) **76**, 51 (1991).

(3) Y. Sunatsuki, Y. Ikuta, N. Matsumoto, H. Ohta, M. Kojima, S. Iijima, S. Hayami, Y. Maeda, S. Kaizaki, F. Dahan, and J.-P. Tuchagues, Angew. Chem. Int. Ed. **42**, 1614 (2003).

(4) Y. Ikuta, M. Ooidemizu, Y. Yamahata, M. Yamada, S. Osa, N. Matsumoto, S. Iijima, Y. Sunatsuki, M. Kojima, F. Dahan, and J.-P. Tuchagues, Inorg. Chem. **42**, 7001 (2003).

(5) M. Yamada, M. Ooidemizu, Y. Ikuta, S. Osa, N. Matsumoto, S. Iijima, M. Kojima, F. Dahan, and J.-P. Tuchagues, Inorg. Chem. **42**, 8406 (2003).

(6) Y. Sunatsuki, H. Ohta, M. Kojima, Y. Ikuta, Y. Goto, N. Matsumoto, S. Iijima, H. Akashi, S. Kaizaki, F. Dahan, and J.-P. Tuchagues, Inorg. Chem. **43**, 4154 (2004).

(7) M. Yamada, E. Fukumoto, M. Ooidemizu, N. Bréfuel, N. Matsumoto, S. Iijima, M. Kojima, N. Re, F. Dahan, and J.-P. Tuchagues, Inorg. Chem. **44**, 6967 (2005).

(8) M. Yamada, H. Hagiwara, H. Torigoe, N. Matsumoto, M. Kojima, F. Dahan, J.-P. Tuchagues, N. Re, and S. Iijima, Chem. Eur. J. **12**, 4536 (2006).

(9) J.-A. Real, H. Bolvin, A. Bousseksou, A. Dworkin, O. Kahn, F. Varret, and J. Zarembowitch, J. Am. Chem. Soc. **114**, 4650 (1992).

(10) S. Decurtins, P. Gütlich, C. P. Kohler, H. Spiering, and A. Hauser, Chem. Phys. Lett. **105**, 1 (1984).

(11) R. Hinek, H. Spiering, D. Schollmeyer, P. Gütlich, and A. Hauser, Chem. Eur. J. **2**, 1127 (1996).

(12) D. Boinnard, A. Bousseksou, A. Dworkin, J.-M. Savariault, F. Varret, and J.-P. Tuchagues, Inorg. Chem. **33**, 271 (1994).